

Statistical Estimation of Refractivity from Radar Sea Clutter

Caglar Yardim, Peter Gerstoft, William S. Hodgkiss
University of California, San Diego
La Jolla, CA 92093-0238, USA
email: cyardim@ucsd.edu, gerstoft@ucsd.edu,
whodgkiss@ucsd.edu

Ted Rogers
Space and Naval Warfare Systems Center
San Diego, CA 92152, USA
email: trogers@spawar.navy.mil

Abstract—This paper summarizes current developments in the refractivity from clutter (RFC) techniques and describes the global parametrization approach in estimation of the lower atmospheric electromagnetic sea ducts. RFC uses radar clutter to gather information about the environment the radar is operating in. Range and height dependent atmospheric index of refraction (M-profile) is statistically estimated from the sea-surface reflected radar clutter. These environmental statistics can then be used to predict the radar performance by taking multidimensional integrals of the posterior probability density.

All of the following methods use a Bayesian framework and use split-step fast Fourier transform based parabolic equation approximation to the wave equation as the propagation model. Environmental parameters are inverted using genetic algorithms, Markov chain Monte Carlo samplers, and a hybrid genetic algorithm - Markov chain Monte Carlo technique. The methods are compared with respect to their estimated maximum a posteriori accuracy, speed and ability to sample correctly from posterior density. The inversion algorithms are implemented on S-band radar sea-clutter data from 1998 Wallops Island, Virginia experiment. Reference data are measured as range-dependent refractivity profiles obtained with a helicopter. The inversions are assessed by comparing the propagation predicted from the radar-inferred refractivity profiles and from the helicopter profiles.

I. INTRODUCTION

Non-standard electromagnetic propagation due to formation of lower atmospheric sea ducts is a common occurrence in maritime radar applications. Under these conditions, some fundamental system parameters of a sea-borne radar can significantly deviate from their original values specified assuming standard-air (0.118 M-units/m) conditions. These include the variation in the maximum operational range, creation of regions where the radar is practically blind (radar holes), and increased sea surface clutter (1). Therefore, it is important to predict the real-time environment the radar is operating in so that the radar operator will at least know the true system limitations and in some cases even compensate for it.

Evaporation and surface-based ducts are associated with increased sea clutter due to the heavy interaction between the sea surface and the electromagnetic signal trapped within the duct. However, this unwanted clutter is a rich source of information about the environment and can be used to determine the local atmospheric conditions. This can be a valuable addition to other more conventional techniques such as radiosondes, rocketsondes, microwave refractometers and meteorological

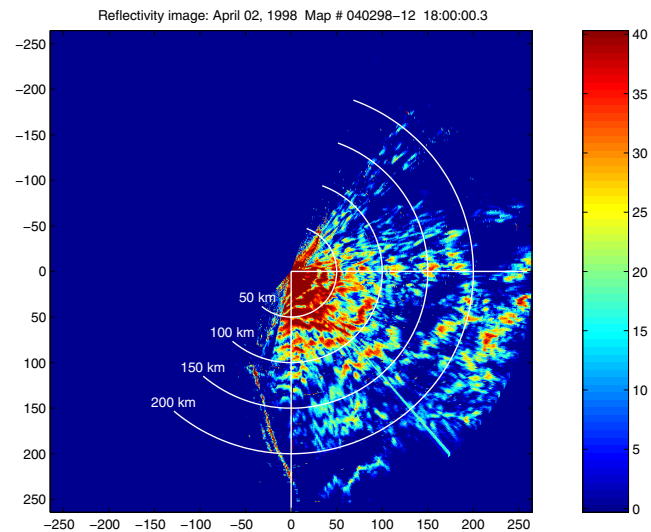


Fig. 1. Clutter map from the SPANDAR radar corresponding to Wallops run 12 with 0° elevation angle.

models such as the Coupled Ocean/Atmospheric Mesoscale Prediction System (COAMPS) that give M-profile forecasts [1]–[4]. There are also other promising techniques that can refer the refractivity using lidar [5] and GPS [6] measurements. In a Bayesian framework, the results of one or several of these techniques above and regional duct statistics [7] can be coupled with the clutter inversion to improve the overall estimation quality. An attractive feature of inferring refractivity from sea surface clutter is that it does not use additional hardware or extra meteorological/electromagnetic measurements. It extracts the information from the radar clutter obtained during normal radar operation, which usually is readily available both as a function of range, direction and time. For a fast inversion algorithm, a near-real-time M-profile structure is obtained. For a fast inversion algorithm, a near-real-time M-profile structure is obtained. The need for a fast algorithm that updates the environmental estimates at intervals of 30 min. or less is evident from [8], where the RMS error in propagation factor exceeds 6 dB after 30 min., due to temporal decorrelation.

Various techniques that estimate the M-profile using radar clutter return are proposed by [9]–[15]. Most of these refractiv-

ity from clutter (RFC) techniques use an electromagnetic fast Fourier transform (FFT) split-step parabolic equation (SSPE) approximation to the wave equation [16], [17], whereas some also make use of ray-tracing techniques. While [9] exclusively concerns evaporation duct estimation, other techniques are applicable to both evaporation, surface-based and mixed type of ducts that contain both an evaporation section and an surface-based type inversion layer. [15] exploits the inherent Markovian structure of the FFT parabolic equation approximation and uses a particle filtering approach, whereas [12] uses rank correlation with ray tracing to estimate the M-profile.

In contrast, [10], [11], [14] and [18] use global parameterization within a Bayesian framework. Since the unknown model parameters are defined as random variables in a Bayesian framework, the inversion results will be in terms of the means, variances and marginal, as well as the n -dimensional joint posterior probability distributions, where n is the number of unknown duct parameters. This gives the user not only the ability to obtain the maximum *a posteriori* (MAP) solution, but also the prospect of performing statistical analysis on the inversion results and the means to convert these environmental statistics into radar performance statistics. These statistical calculations can be performed by taking multi-dimensional integrals of the joint PPD. [10] uses genetic algorithms to estimate the MAP solution. However, no statistical analysis is performed since classical GA is not suitable for the necessary integral calculations. While [11] uses importance sampling, [14] uses Markov chain Monte Carlo (MCMC) samplers to perform the MC integration [19], [20]. Although they provide the means to quantify the impact of uncertainty in the estimated duct parameters, they require large numbers of forward model runs and hence they lack the speed to be near-real-time methods and are not suitable for models with large numbers of unknowns.

A hybrid GA-MCMC method based on the nearest neighborhood algorithm (NA) [21] has been implemented in [18]. It can be classified as an improved GA method, which improves integral calculation accuracy through hybridization with a MCMC sampler. Since the number of forward model samples is based on GA, it requires fewer samples than a MCMC, enabling inversion of atmospheric models with higher complexity with larger number of unknowns.

II. THEORY

To formulate the problem, a Bayesian framework is adopted, where the M-profile model and the radar measured sea-surface clutter data are denoted by the vectors \mathbf{m} and \mathbf{d} , respectively. An electromagnetic FFT-SSPE is used to propagate the field in an environment given by \mathbf{m} and obtain synthetic clutter returns $f(\mathbf{m})$. Since the unknown environmental parameters \mathbf{m} are assumed to be random variables, the solution to the inversion is given by their joint posterior probability distribution function (PPD or $p(\mathbf{m}|\mathbf{d})$). More theory can be found in [10], [11], [14], [18], each one corresponding for one of the methods summarized here. Bayes' formula can be used to write the

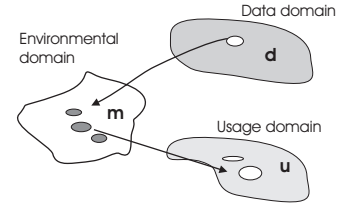


Fig. 2. An observation \mathbf{d} is mapped into a distribution of environmental parameters \mathbf{m} that potentially could have generated it. The environmental parameters are then mapped into the usage domain \mathbf{u} .

PPD as

$$p(\mathbf{m}|\mathbf{d}) = \frac{\mathcal{L}(\mathbf{m})p(\mathbf{m})}{\int_{\mathbf{m}'} \mathcal{L}(\mathbf{m}')p(\mathbf{m}')d\mathbf{m}'}, \quad (1)$$

where $p(\mathbf{m})$ is the prior probability distribution function (pdf) of the parameters. Any information obtained from other methods and regional duct statistics can be incorporated in this step as a prior belief. Since this paper investigates the ability to infer M-profiles using RFC, a uniform prior is used. However, it is possible to include statistical meteorological priors from studies such as [7], for some of the parameters (e.g. the duct height).

Assuming a zero-mean Gaussian error between the measured and modeled clutter, the likelihood function is given by

$$\begin{aligned} \mathcal{L}(\mathbf{m}) &= (2\pi)^{-N_R/2} |\mathbf{C}_d|^{-1/2} \\ &\times \exp \left[-\frac{(\mathbf{d} - f(\mathbf{m}))^T \mathbf{C}_d^{-1} (\mathbf{d} - f(\mathbf{m}))}{2} \right], \end{aligned} \quad (2)$$

where \mathbf{C}_d is the data error covariance matrix, $(\cdot)^T$ is the transpose and N_R is the number of range points used (length of the data vector, \mathbf{d}). Further simplification can be achieved by assuming that the errors are spatially uncorrelated with identical distribution for each data point forming the vector \mathbf{d} . For this case, $\mathbf{C}_d = \nu \mathbf{I}$, where ν is the variance and \mathbf{I} the identity matrix. Then the equation can be simplified to

$$p(\mathbf{m}|\mathbf{d}) \propto p(\mathbf{m}) \left[\frac{N_R}{2\pi e \phi(\mathbf{m})} \right]^{N_R/2} \quad (3)$$

$$\phi(\mathbf{m}) = (\mathbf{d} - f(\mathbf{m}))^T (\mathbf{d} - f(\mathbf{m})). \quad (4)$$

Having defined the posterior density, any statistical information about the unknown environmental and radar parameters can now be calculated by taking these multi-dimensional integrals:

$$\mu_i = \int \dots \int m'_i p(\mathbf{m}'|\mathbf{d}) d\mathbf{m}' \quad (5)$$

$$\sigma_i^2 = \int \dots \int (m'_i - \mu_i)^2 p(\mathbf{m}'|\mathbf{d}) d\mathbf{m}' \quad (6)$$

$$p(m_i|\mathbf{d}) = \int \dots \int \delta(m'_i - m_i) p(\mathbf{m}'|\mathbf{d}) d\mathbf{m}' \quad (7)$$

where μ_i , σ_i^2 , $p(m_i|\mathbf{d})$ are posterior means (Bayesian minimum mean square error (MMSE) estimate), variances, and marginal PPD's of M-profile parameters.

Probability distributions of parameters of interest to a radar operator are calculated in a similar fashion [11]. Assume that u is such a parameter-of-interest (e.g. propagation factor), which naturally is some function $u = g(\mathbf{m})$ of the radar environment \mathbf{m} (Fig. 2). A statistical analysis of u can be carried out by computing the following MC integration

$$p(u|\mathbf{d}) = \int \dots \int \delta(u - g(\mathbf{m}')) p(\mathbf{m}'|\mathbf{d}) d\mathbf{m}'. \quad (8)$$

III. SELECTION OF SAMPLER/OPTIMIZER

The question is about how to efficiently compute these multi-dimensional integrals and MAP solutions. The following list summarizes the techniques that have been used in previous work:

- Genetic algorithms (GA) is used in [10] to successfully compute the MAP solution. Among all the following methods GA is the fastest method in obtaining the MAP. However, it fails to obtain PPD so no integral calculation can be performed.
- Importance sampling (IS) is used in [11]. This allows computation of the necessary posterior integrals without needing to sample from the PPD. It is accurate as long as the prior is not significantly different from the PPD since it gathers the samples necessary for MC integration from the prior.
- Markov chain Monte Carlo (MCMC) samplers are used in [14]. MCMC allows sampling directly from the PPD and hence provides the best estimates of the integral required. However it requires a lot of samples to converge.
- Hybrid GA–MCMC method is used in [18]. This technique is a hybrid between the fastest and the most accurate technique, trying to get reasonably integral calculations using much less forward model runs, typically on the order of a GA run. It uses Voronoi decomposition to approximate the PPD using a typical GA run and then run a MCMC on this approximate PPD minimizing the parabolic equation calculations.

The hybrid method can be summarized by the following steps:

- 1) *GA*: Run a classical GA, minimizing the misfit $\phi(\mathbf{m})$, save all the populations (sampled model vectors) and their likelihood values. MAP solution is obtained as the best fit model vector.
- 2) *Voronoi Decomposition and Approximate PPD*: Using the GA samples $\{\mathbf{m}^i\}$ and their corresponding $p(\mathbf{m}^i|\mathbf{d})$ construct the Voronoi cell structure and create the approximate PPD, $\hat{p}(\mathbf{m}|\mathbf{d})$.
- 3) *Gibbs Resampling*: Run a fast GS on the approximate PPD. No forward modeling is needed.
- 4) *MC Integral Calculations*: Calculate the Bayesian minimum mean square estimate (MMSE), variance and posterior distributions of desired environmental parameters, statistics for the end-user parameters, such as propagation loss L , propagation factor F , coverage diagrams, statistical radar performance prediction, such as the

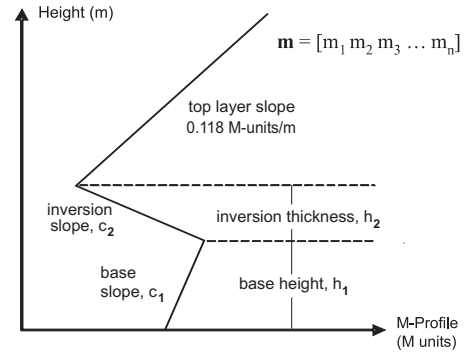


Fig. 3. Four-parameter range-independent tri-linear M-profile.

probability of detection and false alarm using (5) – (7), and (8) using MC integration.

IV. EXAMPLES

Three examples are presented in this section. The first shows how to estimate MC integral using the importance sampling, the second compares GA, MCMC and the hybrid methods and the last one analyzes a range-dependent profile with a high number of parameters using the hybrid method.

The first example is created using a range-dependent 8 parameter surface-based duct formed using 2 tri-linear M-profiles at 0 and 100 km, where a typical tri-linear profile is shown in Fig. 3. It is taken from [11]. The unknown model parameters are the slope and height of the base layer (c_1 and h_1) and the slope and thickness of the inversion layer (c_2 and h_2). Since the RFC is insensitive to the M-profile parameters above the duct, the top layer slope corresponds to standard atmosphere. The data are generated based on the helicopter measured range-dependent refractivity profile (run 7) for the Wallops 98 experiment. Then samples are drawn from the prior density given in Fig. 4 and their likelihood are computed using (2). Any required parameter can now be computed by using these likelihood values as appropriate weight factors in integral calculations. 1-D and 2-D PPD estimate is given in Fig. 5. Note that any integral using importance sampling will be less accurate if prior is too different with respect to the PPD such as the third parameter (slope 1) in this examples.

The second example is [18] a 4 parameter surface-based duct. This example compares GA, MCMC and the hybrid methods in terms of their computational complexity, MAP accuracy, and PPD estimation accuracy. It computes the true values using exhaustive search to provide a benchmark. 1-D marginal model parameter PPD's are given in Fig. 6 for (a) exhaustive search, (b) Metropolis-Hastings sampler (conventional MCMC), (c) pure GA, and (d) hybrid GA-MCMC method, respectively. Exhaustive search results are assumed to have a dense enough grid to give the true distributions and will be used as the benchmark. As expected, the Gibbs sampler results are close to the true distribution but requires 70×10^3 (70k) samples to converge. The GA uses 15k samples (5k is enough to get the MAP solution). The distributions are clearly not accurate, however, as a global optimizer it does

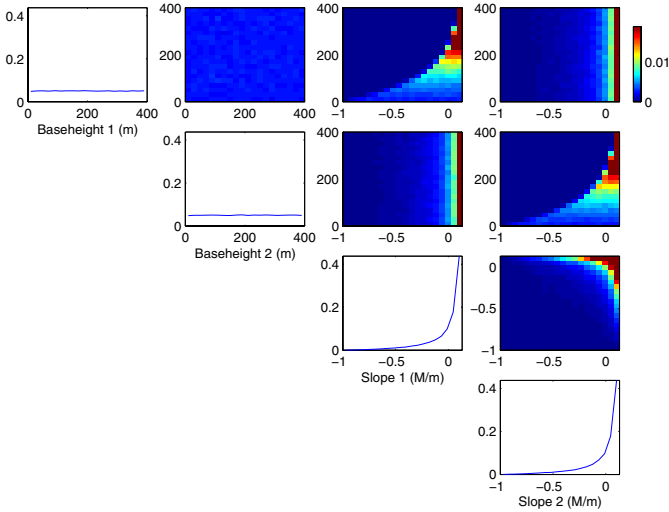


Fig. 4. Prior probability distribution for the base height and slope at 0 and 100 km range. Along the diagonal the marginal for each parameter is plotted, and above the diagonal show the 2D marginals (red indicates higher probability). The distributions below the diagonal are symmetric with those above.

its job of minimizing $\phi(\mathbf{m})$ and obtaining MAP very fast. The GA sample histograms presented here are not unique. Every GA run will result in a different set of curves, without any specific sampling density $p_s(\mathbf{m}|\mathbf{d})$. The hybrid method actually uses the 15k GA samples obtained in (c) to perform the Voronoi decomposition. When a fast Gibbs resampling is performed on the approximate PPD, results comparable to the conventional MCMC solution is obtained. A Gibbs resampling of just 20k samples is sufficient to calculate the MC integral accurately (40k is used in (d)). It should be noted that (d) is extracted using the forward model samples obtained in (c). All information about the search space comes from the GA samples and the hybrid method makes the information hidden in the GA set available for MC integration through Voronoi decomposition.

The final example is taken from [18]. To further demonstrate the capabilities and limitations of the hybrid method, a range-dependent environmental model comprising of sixteen parameters is employed during the inversion of the 1998 Wallops island experiment data. A range dependent inversion is achieved by defining vertical, four-parameter tri-linear M-profiles at certain ranges (0, 20, 40, and 60 km) and linearly interpolating the parameters in between. Slopes for both the first and the second layers can be negative and positive to give more flexibility in the modeling. Hence, they are only referred to by their layer numbers. Layer slopes at different ranges can vary independent of each other. On the contrary, a Markovian structure is used for the layer heights with a maximum of 30 m variation relative to the height value at the previous range. The height values except for the first profile are difference in meters between the layer thicknesses of two consecutive profiles, so they can be ± 30 m.

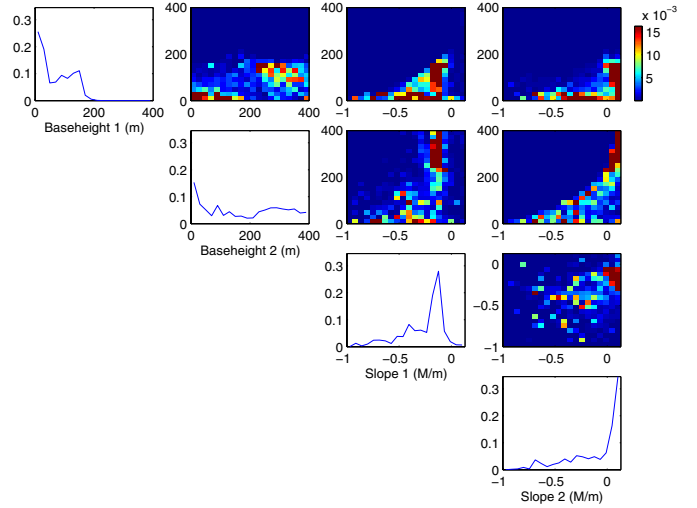


Fig. 5. Posterior probability distribution for the base height and slope at 0 and 100 km range. Along the diagonal the marginal for each parameter is plotted, and above the diagonal show the 2D marginals (red indicates higher probability). The distributions below the diagonal are symmetric with those above.

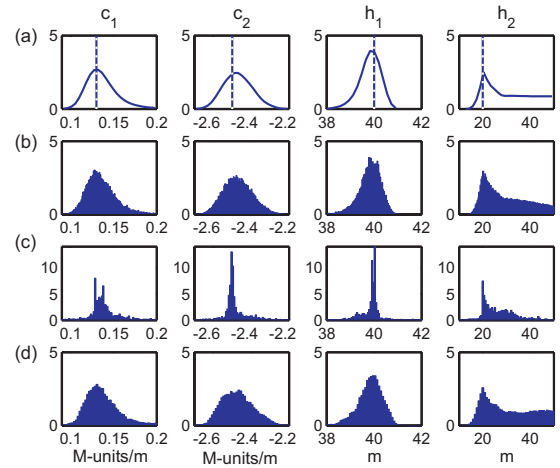


Fig. 6. Marginal posterior probability distributions for the synthetic test case. Vertical lines show the true values of the parameters. (a) Exhaustive search, (b) Metropolis sampler (MCMC), (c) GA, and (d) hybrid GA-MCMC using 15k GA and 40k Gibbs samples.

Only 13 out of 16 parameters are given in Fig. 7(a). The height parameters of the second layers m_8 , m_{12} , and m_{16} are omitted, as they are not important. Since clutter is mostly due to the EM signal trapped inside the duct, it mostly contains information about the parameters inside the duct, making the second layer heights poorly determined except for very close ranges. To demonstrate this, normalized error function $\phi(\mathbf{m})/\phi(\mathbf{m}_{MAP})$ for various conditional planes are given in Fig. 7(b). These curves are obtained by fixing other parameters to their MAP values and calculating $\phi(\mathbf{m})$ while varying only two parameters at a time. Except for the bottom plots all the plots show quickly varying complex patterns whereas the last ones are flat since the horizontal axis for these is either m_8 ,

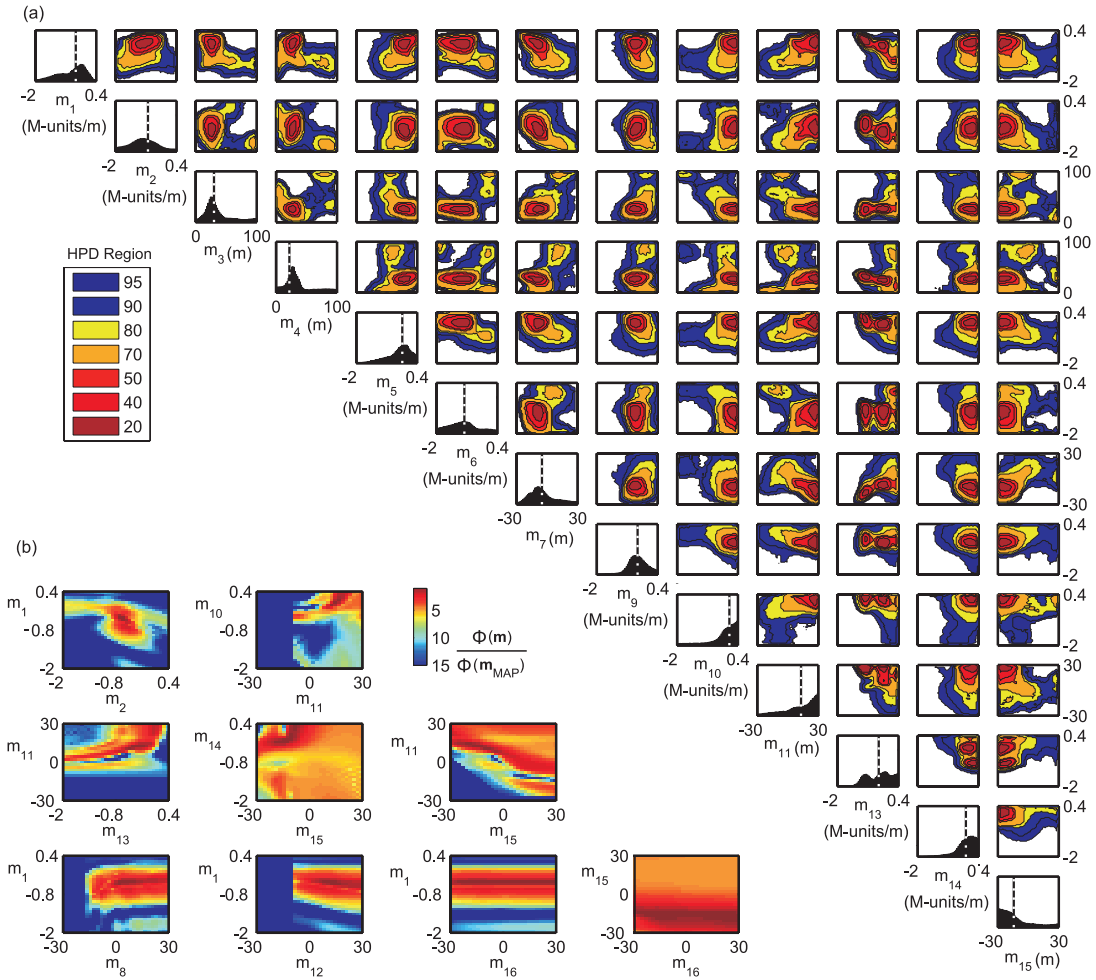


Fig. 7. Marginal and conditional distributions. (a) 1-D (diagonal) and 2-D (upper diagonal) posterior probability distributions in terms of percent HPD, for the range-dependent SPANDAR data inversion. 13 parameters (m_{1-7} , m_{9-11} , m_{13-15}) out of 16 are given. Vertical lines in the 1-D plots show the GA MAP solution. (b) Normalized error function for various conditional planes. Each 2-D plot is obtained by fixing the other 14 parameters to their MAP values.

m_{12} , or m_{16} (second layer heights). Some plots such as m_1 vs. m_{12} have zero likelihood regions since the height parameters which are Δh at 20, 40, and 60 km cannot be less than values that would make the actual layer thickness negative.

The environmental statistics can be projected into statistics for user parameters (see Section II). One typical parameter of interest to an end-user is the propagation factor F . The results in Fig. 8 are obtained from the parameter PPD in Fig. 7. It shows the PPD for F at ranges (a) 18, (b) 40, and (c) 60 km. Contour plots show the PPD of F for height values between 0–200 m, with the MAP solution (dashed white). Horizontal lines represent the three altitudes analyzed in detail in the small plots shown next to the color plots. Comparison of plots at the same range and different altitudes reveals some important aspects of RFC.

First, the propagation factor PPDs inside the duct (at 20 m) are sharper than those outside the duct (100 and 180 m). This is expected since we used the sea clutter which is usually affected only by the lower portions of the atmosphere to infer the environment. The PPDs do also become flatter

with increasing range. Note how the error made by using the standard atmospheric assumption (black dashed lines) increases with range, especially inside the duct. At $[H, R] = [20 \text{ m}, 18 \text{ km}]$ all three curves (MAP, helicopter profile, and standard atmosphere) are almost identical whereas standard atmospheric assumption leads to more than 40 dB error for $[H, R] = [20 \text{ m}, 60 \text{ km}]$ while MAP and helicopter profile comply with the underlying PPD. Finally, the difference between the helicopter profile and MAP tends to be larger outside the duct.

V. CONCLUSION

Various RFC methods has been summarized. These methods have been used for statistical sea-borne radar performance estimation under non-standard propagation conditions. Statistical refractivity-from-clutter (RFC) inversion is used to gather information about the environment, such as the range-dependent vertical structure of the atmospheric index of refraction, and then these environmental uncertainties are used to estimate parameters-of-interest to be used by the radar operator.

As a forward model, a fast Fourier transform split-step parabolic equation (FFT-SSPE) approximation to the wave

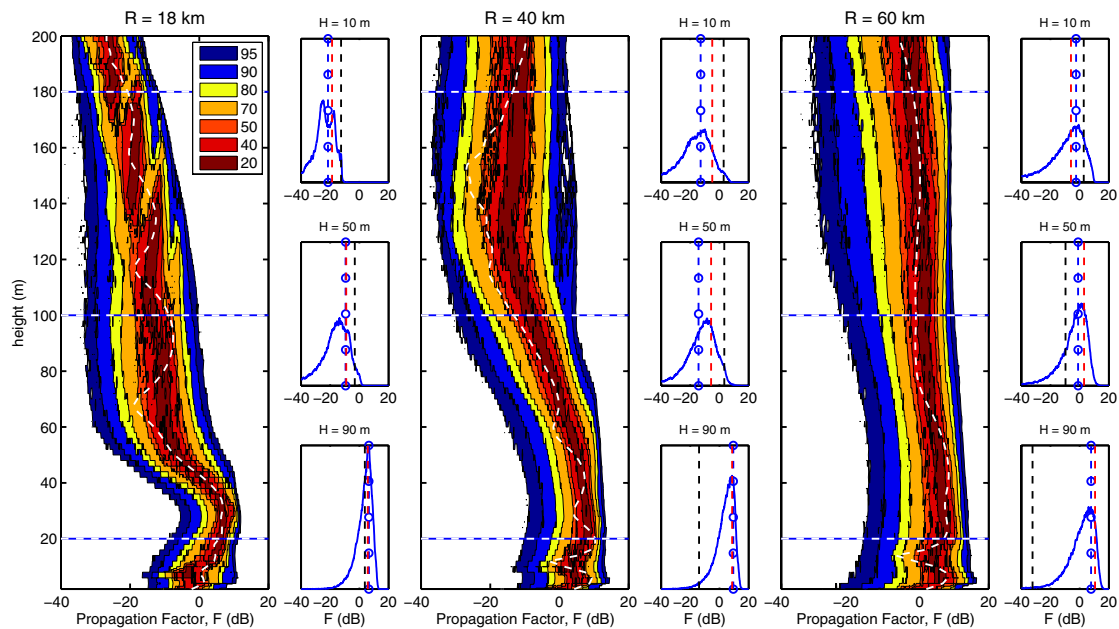


Fig. 8. Posterior probability densities for propagation factor F at three different ranges: (a) 18, (b) 40, and (c) 60 km. Color plots show the PPD of F for height values between 0 m and 200 m in terms of percent HPD, with the MAP solution (dashed white). Horizontal lines represent the three altitudes analyzed in detail in the small plots shown next to the color plots at heights 180, 100, and 20 m, respectively from top to bottom. Vertical lines in the small plots represent the values of F at the corresponding height and range for the MAP solution (blue line with circles), helicopter measurement (red), and standard atmospheric assumption (black).

equation was used to propagate the electromagnetic signal in complex environments. The hybrid method uses fewer forward model calculations than a classical MCMC while obtaining more accurate distributions than GA. This enables inclusion of more unknown parameters and range-dependent atmospheric models. The capabilities of the technique were illustrated for a sixteen dimensional range-dependent inversion.

VI. ACKNOWLEDGMENT

This work was supported by the Office of Naval Research under grant N00014-05-1-0369.

REFERENCES

- [1] J. R. Rowland and S. M. Babin, "Fine-scale measurements of microwave profiles with helicopter and low cost rocket probes," *Johns Hopkins APL Tech. Dig.*, vol. 8 (4), pp. 413–417, 1987.
- [2] E. R. Thews, "Timely prediction of low-altitude radar performance in operational environments using *in situ* atmospheric refractivity data," *IEE Proc.*, vol. 137 (F-2), pp. 89–94, 1990.
- [3] R. M. Hodur, "The naval research laboratory's coupled ocean/atmosphere mesoscale prediction system (COAMPS)," *Monthly Weather Review*, vol. 125(7), pp. 1414–1430, 1996.
- [4] M. I. Skolnik, *Introduction to Radar Systems*, 3rd ed. New York: McGraw-Hill, 2001.
- [5] A. Willitsford and C. R. Philbrick, "Lidar description of the evaporative duct in ocean environments," vol. 5885. Proceedings of SPIE, Bellingham, WA, September 2005.
- [6] A. R. Lowry, C. Rocken, S. V. Sokolovskiy, and K. D. Anderson, "Vertical profiling of atmospheric refractivity from ground-based GPS," *Radio Science*, vol. 37(3), pp. 1041–1059, 2002, doi:10.1029/2000RS002565.
- [7] S. M. Babin, "Surface duct height distributions for Wallops island, Virginia, 1985–1994," *Journal of Applied Meteorology*, vol. 35 (1), pp. 86–93, 1996.
- [8] L. T. Rogers, "Effects of variability of atmospheric refractivity on propagation estimates," *IEEE Trans. Antennas Propagat.*, vol. 44 (4), pp. 460–465, 1996.
- [9] L. T. Rogers, C. P. Hattan, and J. K. Stapleton, "Estimating evaporation duct heights from radar sea echo," *Radio Science*, vol. 35 (4), pp. 955–966, 2000, doi:10.1029/1999RS002275.
- [10] P. Gerstoft, L. T. Rogers, J. Krolik, and W. S. Hodgkiss, "Inversion for refractivity parameters from radar sea clutter," *Radio Science*, vol. 38 (3), pp. 1–22, 2003, doi:10.1029/2002RS002640.
- [11] P. Gerstoft, W. S. Hodgkiss, L. T. Rogers, and M. Jablecki, "Probability distribution of low altitude propagation loss from radar sea-clutter data," *Radio Science*, vol. 39, pp. 1–9, 2004, doi:10.1029/2004RS003077.
- [12] A. Barrios, "Estimation of surface-based duct parameters from surface clutter using a ray trace approach," *Radio Science*, vol. 39 RS6013, pp. 1–15, 2004, doi:10.1029/2003RS002930.
- [13] L. T. Rogers, M. Jablecki, and P. Gerstoft, "Posterior distributions of a statistic of propagation loss inferred from radar sea clutter," *Radio Science*, vol. 40 (6), pp. 1–14, 2005, doi:10.1029/2004RS003112.
- [14] C. Yardim, P. Gerstoft, and W. S. Hodgkiss, "Estimation of radio refractivity from radar clutter using Bayesian Monte Carlo analysis," *IEEE Trans. Antennas Propagat.*, vol. 54(4), pp. 1318–1327, 2006.
- [15] S. Vasudevan, R. Anderson, S. Kraut, P. Gerstoft, L. Rogers, and J. Krolik, "Recursive Bayesian electromagnetic refractivity estimation from radar sea clutter," *Radio Science*, in press.
- [16] A. E. Barrios, "A terrain parabolic equation model for propagation in the troposphere," *IEEE Trans. Antennas Propagat.*, vol. 42 (1), pp. 90–98, 1994.
- [17] M. Levy, *Parabolic Equation Methods for Electromagnetic Wave Propagation*. London, United Kingdom: The Institution of Electrical Engineers, 2000.
- [18] C. Yardim, P. Gerstoft, and W. S. Hodgkiss, "Statistical maritime radar duct estimation using a hybrid genetic algorithms – Markov chain Monte Carlo method," *Radio Science*, in press.
- [19] J. J. K. Ó Ruanaidh and W. J. Fitzgerald, *Numerical Bayesian Methods Applied to Signal Processing*, ser. Statistics and Computing Series. New York: Springer-Verlag, 1996.
- [20] D. J. C. MacKay, *Information Theory, Inference and Learning Algorithms*. Cambridge, United Kingdom: Cambridge University Press, 2003.
- [21] M. Sambridge, "Geophysical inversion with a neighborhood algorithm - II. appraising the ensemble," *Geophys. J. Int.*, vol. 138, pp. 727–746, 1999.